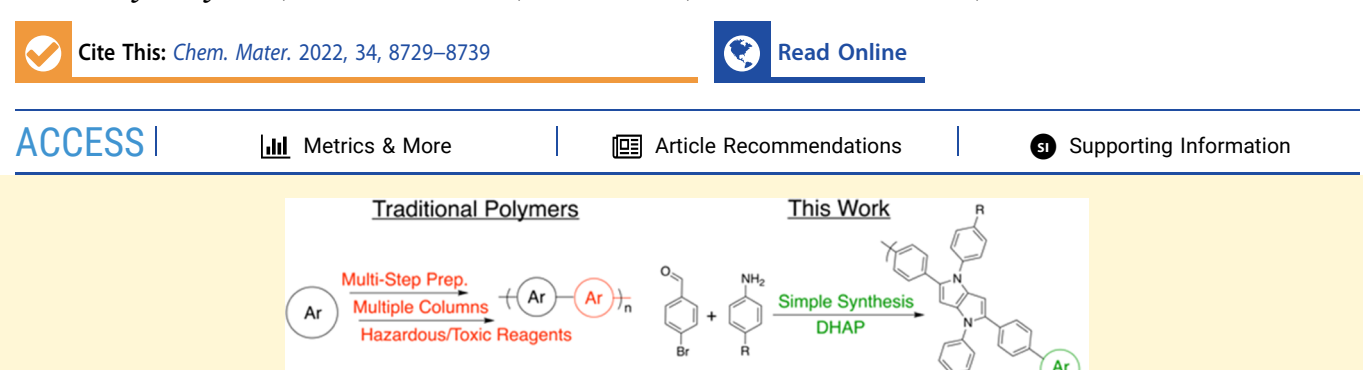


pubs.acs.org/cm Article

Simple Synthesis of Conjugated Polymers Enabled via Pyrrolo[3,2-b]pyrroles

Kenneth-John J. Bell, Allison M. Kisiel, Evan Smith, Aimée L. Tomlinson, and Graham S. Collier*



ABSTRACT: Accessing conjugated polymers suitable for applications ranging from organic photovoltaics to bioelectronics through simple synthetic protocols is desirable for the conjugated polymer community, as many polymer systems that meet device performance metrics require arduous synthetic protocols. To simplify and minimize monomer and polymer synthetic steps, a dibrominated dihydropyrrolopyrrole was synthesized in air using a single synthetic step and did not require column chromatography for purification. Subsequently, the first example of an electron-rich pyrrolopyrrole monomer being polymerized is accomplished via direct arylation polymerization using a dioxythiophene comonomer to access an alternating copolymer in a total of three synthetic steps. The resulting copolymer exhibits absorbance in the high-energy portion of the visible spectrum in solution and the solid state, a relatively low onset of oxidation (~0.6 V vs Ag/AgCl), and yellow-to-black electrochromism. Finally, the synthetic complexity is calculated, and the pyrrolopyrrole-co-dioxythiophene polymer is less synthetically complex when compared to many conjugated polymers that find applicability in organic photovoltaics and electrochromism. These findings demonstrate the viability of incorporating dihydropyrrolopyrroles into the repeat unit structure of conjugated polymers via metal-catalyzed cross-coupling reactions and highlight their potential to offer a synthetically simple alternative to current state-of-the-art conjugated polymers.

■ INTRODUCTION

Conjugated polymers are critical materials in various types of organic electronic devices, such as organic photovoltaics (OPVs), organic light-emitting diodes (OLEDs), or electrochromics, but one substantial limitation to their widespread utilization in these applications is the arduous and complex nature of their synthesis. Typically, the synthesis of high-performance conjugated polymers requires numerous synthetic steps, including air and moisture-free environments or cryogenic conditions, harsh/toxic reagents, and rigorous purifications during the preparation of their monomeric building blocks. Besearchers are aware of this drawback, and thus, attention has been shifted toward conjugated polymers made using simple chemistries.

As researchers have shifted their focus to simplifying the synthesis of conjugated polymers, efforts to quantify "how simple?" have emerged. First, Po and co-workers defined the synthetic complexity of a polymer as being dependent on five parameters, including the number of synthetic steps (NSS), the reciprocal yield of monomers (RY), the number of operations required for purification of monomers (NUO), the number of column chromatography purifications (NCC), and the number of hazardous materials used (NHC). While this approach has become a useful method for estimating synthetic complexity,

McCulloch and co-workers suggest that there are too many inconsistencies in reported synthetic methods, as well as discrepancies in hazard definitions. Thus, they developed the scalability factor (SF), where the NSS and RY of the synthetic route are the main factors influencing these benchmark calculations. Regardless of the approach used to assess the synthetic complexity of conjugated materials, the emphasis on reducing the number of synthetic steps while using starting materials "that could be found in the market in quantities sufficient to produce hundreds of kilograms of polymers" provides motivation to explore new structural design motifs with simple chemistries.

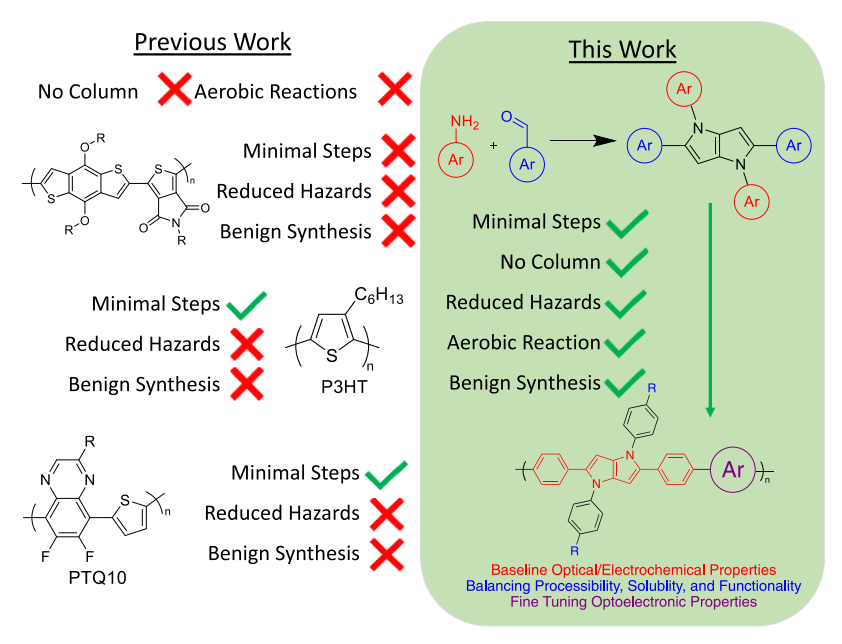
One example of these efforts is reflected by the polymer known as PTQ10, which can be accessed in three (3) synthetic steps while achieving a power conversion efficiency (PCE) of $\sim 16\%$ when incorporated into bulk heterojunction blends with a non-fullerene acceptor. ⁹⁻¹¹ While this is a significant

Received: June 23, 2022 Revised: September 15, 2022 Published: September 27, 2022





Scheme 1. Representative Structures of Traditionally Studied Conjugated Polymers and the Attributes of Utilizing DHPP Copolymers



achievement for minimizing synthetic steps and maintaining device performance metrics, there are multiple drawbacks. Specifically, the synthesis of PTQ10 monomers involves the use of potassium tert-butoxide, which is a flammable solid that is classified as self-heating in large quantities, starting material and precursors are expensive, and polymers are synthesized via Stille cross-coupling polymerizations, which generate stoichiometric amounts of trialkyltin waste. Additionally, You and coworkers performed a cost analysis of PTQ10 and suggested that current synthetic approaches are cost-prohibitive. These drawbacks limited the scalability and commercial manufacturing of this polymer and motivated the pursuit of alternative synthetic approaches that ultimately reduced the price per gram to ~1/7th the original cost. 12 Additional approaches for accessing structurally simpler conjugated copolymers involve using commercially available monomers such as bithiophene or ester- and alkyl-functionalized monomers that require fewer synthetic steps. 13-18 Recently, Marks and co-workers also reported a simpler synthesis of naphthalene diimide and isoindigo copolymers that were utilized in all-polymer solar cell devices. 19 Although these monomers require fewer synthetic steps, air-free and sometimes cryogenic conditions are still required. These limitations reinforce the need to explore new monomer designs that rely on simplified and scalable chemistries that yield useful conjugated polymers.

When considering synthetic approaches that simplify syntheses, it is advantageous to eliminate or reduce procedures that require air-free reactions, produce toxic byproducts, require chromatography for purification, and use high temperature/pressure or cryogenic reaction conditions. With this in mind, pyrrolo[3,2-b]pyrrole (DHPP) is a building block that meets these criteria while also representing a highly tailorable chromophore with properties amendable to technologically relevant applications. DHPPs (Scheme 1) represent a class of electron-rich, 10 π -electron chromophores that are easily synthesized in a single step and are highly tailorable through simple structural modification. Until recently, efficient protocols to synthesize DHPPs had remained elusive when

Gryko and co-workers serendipitously discovered²⁰ that DHPPs were quickly formed by reactions between aldehydes, anilines, and butanedione in the presence of acetic acid. Moreover, and as implied in Scheme 1, Gryko's synthesis of DHPPs can be performed in air and does not require column chromatography for purification.²¹ This discovery has spurred research focused on optimizing reaction conditions and expanding functional group tolerance, which has allowed families of chromophores with diverse functionality to be readily synthesized.^{22–24} The variety of functional groups is important, as it has allowed chromophores with tunable optical properties,^{25,26} aggregation-induced emission,^{27,28} and two-photon fluorescence,²⁹ to be made.

Beyond fundamental manipulation of optical properties, the facile tunability and versatility motivate studying molecular DHPPs for various optoelectronic applications. As it relates to photovoltaic studies, Dominguez and co-workers developed a small-molecule acceptor-donor-acceptor system by functionalizing the 2- and 5-position aryl rings of DHPP with dicyanovinylenes. This chromophore was used as the lightharvesting material in OPV devices and achieved a maximum PCE of 1.06%.³⁰ Other efforts have involved extending the conjugated pathway between the DHPP core and acceptor region through the addition of thienyl or carbazole moieties, which resulted in a PCE of up to 6.56% when using these dyes in a dye-sensitized solar cell (DSSC).31 Zhang et al. synthesized an acceptor-donor-acceptor DHPP using benzothiadiazole at the 2,5-aryl position to yield a chromophore exhibiting red emission with a solution fluorescence quantum yield (Φ) of 57% and a maximum external quantum efficiency (EQE) of 3.4% in an OLED device. 32 Finally, DHPPs have been used in resistive memory devices³³ and organic photodetectors.³⁴ While these examples highlight the potential applicability of molecular DHPP materials, there is not an example of DHPPs being directly incorporated into a polymeric main chain; thus, fundamental structure-property relationships of polymer-containing DHPPs are unknown.

Scheme 2. Synthesis of Br_2DHPP Via the Fe-Catalyzed Multicomponent Reaction Using *n*-Decylaniline to Construct Monomers That Will Impart Adequate Solubility of Resulting Polymers and a Photograph of ~ 15 g of the Br_2DHPP Monomer Next to a 20 mL Vial to Illustrate Scalability

Motivated by the vast tailorability of DHPP chromophores, combined with their simple synthesis and purification, we hypothesized that DHPP would be a useful monomeric building block for synthesizing conjugated polymers. This approach involves synthesizing a dibrominated DHPP, which enables the synthetically simple DHPP comonomer to participate in Pd-catalyzed polymerizations. Herein, we describe the first example of a DHPP-containing copolymer synthesized via direct heteroarylation polymerization (DHAP) with 3,4-propylenedioxythiophene (ProDOT) as the comonomer. Initial understanding of structure-property relationships of this novel material is investigated by comprehending how monomer structures influence synthetic accessibility and optical, thermal, and electrochemical properties. Additionally, we quantify the synthetic complexity that reveals the first DHPP copolymer to be among the simplest conjugated polymers to be synthesized. As alluded to in Scheme 1, the incorporation of DHPP into polymeric materials offers a readily accessible and tunable scaffold for conjugated polymers without compromising properties commonly associated with solid-state or electrochemical applications. This study demonstrates the ability to incorporate a synthetically simple monomer into the main chain of a polymer repeat unit while simultaneously providing a novel building block that may find utility in next-generation organic materials.

■ EXPERIMENTAL SECTION

Comprehensive details of the experimental approaches are assembled and reported in the Supporting Information. Structure and connectivity of synthesized molecules and polymers were confirmed via ¹H and ¹³C NMR. Spectra were collected using a Bruker Ascend 400 MHz NMR spectrometer. Full characterization, including NMR, elemental analysis, and size-exclusion chromatography (SEC) data, can be found in the Supporting Information. Absorbance properties of molecules and polymers were studied using either a Cary 4000 dualbeam UV-vis spectrophotometer or a Cary 5000 dual-beam UVvis-NIR spectrophotometer. To prepare spray-coated films, polymers were dissolved in toluene with a concentration of 2 mg/mL before deposition onto ITO-coated glass slides with an Iwata airbrush. Electrochemical and spectroelectrochemical measurements performed on the films used an electrolyte solution of 0.5 M tetrabutylammonium hexafluorophosphate (TBAPF₆) in propylene carbonate (PC), ITO/glass (7 × 50 × 0.7 mm³, sheet resistance, R_s 8–12 Ω /sq) as the working electrode, an Ag/AgCl reference electrode (calibrated vs the Fe/Fe⁺ redox couple, $E_{1/2} = 40$ mV), and a Pt flag as the counter electrode.

■ RESULTS AND DISCUSSION

Conjugated polymers are notoriously insoluble, so our initial efforts involved the synthesis of DHPP monomers that will aid in attaining soluble copolymers. These efforts began with attempting to replicate the DHPP synthesis using 4-aminophenol and 4-bromobenzaldehyde, followed by alkylation protocol inspired from the literature procedure reported by Li and co-workers, as shown in Scheme S1.31 The resulting product, (OH)₂DHPP, was obtained with a favorable yield of 55%; however, the subsequent alkylation attempts via Williamson etherification resulted in yields between 5 and 8%. In an effort to improve yields and overall atom economy, 4-aminophenol was replaced with 4-n-decylaniline to access a monomer amendable to Pd-catalyzed polymerizations in one step, in air, and that requires simple purifications (i.e., vacuum filtration). 4-Decylaniline was chosen as it was hypothesized to impart solubility that enables thorough characterization and, eventually, solution processibility of the resulting polymers. Furthermore, as shown in Scheme 2, this change significantly improved the overall yield of the desired monomer from 8 to 49%. The structure and purity of the resulting monomer were verified via ¹H and ¹³C NMR (Figures S2 and S3) and elemental analysis, respectively. After a successful synthesis, the reaction was scaled to 80 mmol to save time on future synthetic efforts as well as to simulate potential industrial scalability. Notably, the product from the 80 mmol reaction does not sacrifice the yield nor purity of the resulting monomer compared to the same monomer isolated from smaller scale reactions and yielded \sim 15 g in a single synthetic step.

Conjugated polymers are traditionally synthesized via Pdcatalyzed cross-coupling reactions, such as Miyaura-Suzuki and Migita-Stille polycondensations, 35,36 but these synthetic strategies suffer restrictive synthetic barriers in their respective procedures, such as monomer stability and potentially costly/ toxic functionalization steps. Stemming from the motivation to simplify polymer synthesis by minimizing preparatory steps, we also are motivated to minimize the use/generation of toxic reagents. To accomplish these goals, we sought to use direct heteroarylation polymerization (DHAP) to access the envisioned synthetically simple conjugated polymers. DHAP is a green alternative polymerization strategy because it minimizes monomer preparation steps while simultaneously minimizing/eliminating toxic reagents by forgoing the need for organometallic functionalities that participate in the transmetalation process of Pd-catalyzed cross-couplings. 37-40 Additionally, DHAP is becoming a robust polymerization strategy

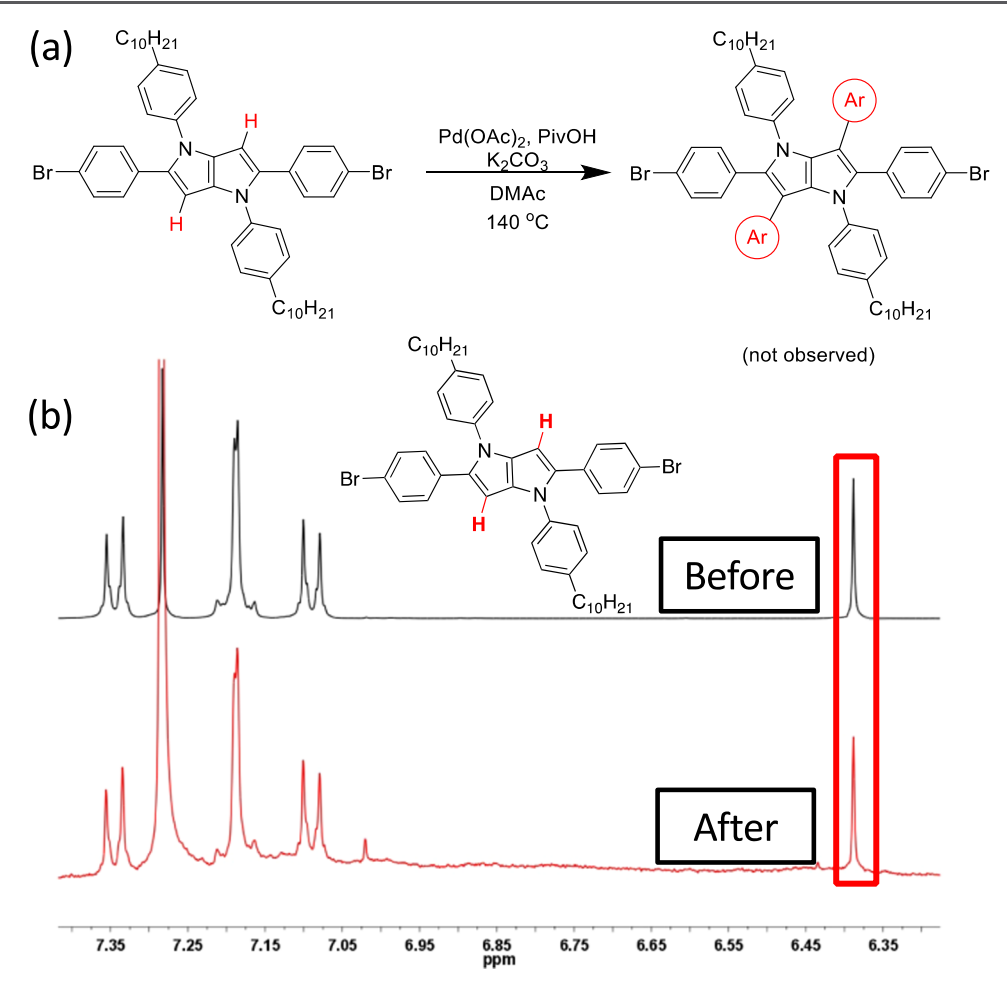


Figure 1. (a) Model reaction to investigate possible 3,6-cross-coupling defects on the DHPP monomer in high dielectric polymerization conditions and (b) 1 H NMR spectra of Br₂DHPP before (black) and after (red) subjecting the monomer to the reaction conditions. The singlet highlighted with the red box \sim 6.37 ppm is unchanged, confirming no C–H cross-coupling reactions occurred on the DHPP scaffold.

that enables accessing low-defect conjugated polymers without sacrificing device performance metrics. 41

Initial polymerization attempts to incorporate DHPP as a comonomer into conjugated polymers were attempted with thienopyrroledione (TPD) due to it being an extensively studied comonomer and its propensity to efficiently participate in DHAP.⁴² These attempts were unsuccessful at obtaining copolymers with suitable solubility in organic solvents, evident by excessive material remaining in the Soxhlet thimble following extraction protocols in addition to bimodal molecular weight distributions measured via size-exclusion chromatography (SEC) (see Figure S5a). The insolubility ultimately prevented a thorough and accurate characterization of polymeric properties and understanding of structureproperty relationships (Figure S5b). These limitations motivated pursuing alternative comonomers to overcome solubility barriers encountered in these initial studies. When considering comonomers for direct arylation polymerizations with DHPP, 3,4-propylenedioxythiophene (ProDOT) appears to be a suitable choice while offering facile tunability and synthetically simple monomers. This motivation stems from its one-step synthesis and ease of functionalization for reactivity with numerous polymerization methods such as Grignard metathesis, oxidative polymerization, and Pd-catalyzed crosscouplings.⁴³ Furthermore, various solubilizing motifs can be installed onto ProDOT in one or two steps via transetherification reactions that utilize commercially available starting materials, such as 2,2-di-*n*-octyl-1,3-propanediol. Due to this tailorability, ProDOT polymers have been used as electroactive materials in various organic electronics such as electrochromics and OPVs. Combined, these characteristics of ProDOT motivated its choice for polymerization with DHPP and enabled understanding structure—property relationships of DHPP-based copolymers.

With the desire to polymerize DHPP with ProDOT, we started with an established DHAP procedure for producing poly(ProDOT)s that uses the high dielectric solvent N₁Ndimethylacetamide (DMAc), palladium(II) acetate (Pd- $(OAc)_2$) as the catalyst, potassium carbonate (K_2CO_3) as the base, and pivalic acid (PivOH) as the proton shuttle while heating the reaction mixture at 140 °C.⁴⁸ It is noteworthy to mention that the 3,6-position hydrogens of DHPP, illustrated as the red protons in Figure 1a, have been shown to participate in direct arylation reactions to access multi-aryl DHPP chromophores, ^{22,26,49} which motivated screening the DHPP monomer in high dielectric DHAP conditions and monitoring for any observable coupling at the 3,6-positions of the pyrrolopyrrole scaffold. Such coupling at the 3,6-position would result in cross-linked polymer or polymers with an appreciable number of β -defects, which may produce insoluble materials or lead to diminished material properties. 27,28 After subjecting the pyrrolopyrrole monomer to the reaction

Scheme 3. Direct Arylation Polymerization for the Synthesis of DHPP-co-ProDOT

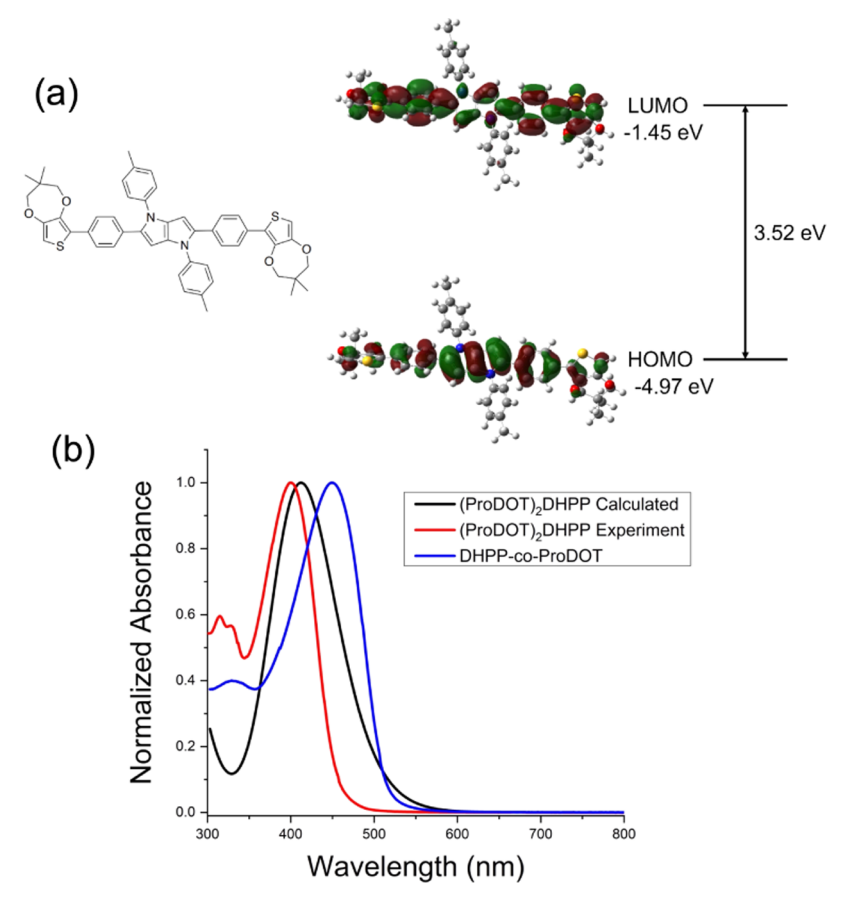


Figure 2. (a) Structure and frontier molecular orbital maps of the $(ProDOT)_2DHPP$ oligomer used for TD-DFT calculations. (b) Normalized UV-vis absorbance spectra of the resulting TD-DFT calculations of a $(ProDOT)_2DHPP$ oligomer (black), a synthesized $(iBuProDOT)_2DecylDHPP$ oligomer in toluene solution (red), and DHPP-co-ProDOT copolymer in toluene solution. The proximity of λ_{max} values of calculated and experimental UV-vis spectra support the level of theory and indicate the effective conjugation length is greater than 5 rings.

conditions mentioned above, the first indication of the absence of cross-coupling defects was from not observing any new spots on thin layer chromatography (TLC). These results were then confirmed with ¹H NMR (vide infra).

Figure 1 shows overlaid ¹H NMR spectra of Br₂DHPP before and after the model reaction. As shown in Figure 1, the lack of change for the singlet at ~6.37 ppm, as well as the absence of new chemical shifts in the aromatic region confirm that no 3,6-coupling was observed and encourage the pursuit of polymerizations using the high dielectric conditions. The established DHAP procedure (Scheme 3) yielded a yellow

polymer with a number-average molecular weight $(M_{\rm n})$ of 10.5 kg/mol and dispersity $(M_{\rm w}/M_{\rm n})$ of 2.0, as determined by SEC vs polystyrene standards using CHCl₃ as the eluent (Figure S6). It is worthy to note that the polymer solutions were difficult to filter through a 0.45 μ m SEC prefilter, likely due to solubility constraints at concentrations commonly used for GPC measurements, ⁵⁰ which may inhibit the accurate estimation of the polymer molecular weight. Nonetheless, polymers with a $M_{\rm n} > 10$ kg/mol are typically considered of sufficient molecular weight such that electronic properties are saturated and result in polymeric systems with appropriate

viscosities needed for solution processing of thin films. ⁴⁷ The resulting polymer retained the pyrrolopyrrole singlet at 6.38 ppm and the singlet at 4.10 ppm, attributed to protons on the propylene bridge of ProDOT, thus confirming the successful incorporation of ProDOT into the polymer in an alternating manner (see Figure S4). As shown in the Experimental Section of the Supporting Information, purity and composition were further verified with elemental analysis that showed similar values for expected and determined atomic compositions. Polymers with high compositional purity are required for accurately determining structure—property relationships, given that residual impurities are known to be detrimental to the performance of organic materials. ^{51–53}

DHPP molecules have been studied for a variety of optical and optoelectronic applications, 25-34 which motivates our investigation of the optical properties of DHPP-co-ProDOT using UV-vis and fluorescence spectroscopies. After the successful synthesis, we first turn to calculations to probe fundamental structural and optical properties. Excited state transitions of a (ProDOT)₂DHPP oligomer were calculated via density functional theory (DFT) geometry optimization, followed by time-dependent density functional theory (TD-DFT), both using the mPW1PBE functional paired with the cc-PVDZ basis set. These parameters were chosen because they have been shown to accurately correlate with calculated and experimental absorbance spectra of ProDOT-containing oligomers. 54,55 Figure 2a and Table S1 summarize the results showing that model oligomers possess wide band gaps (~3.5 eV), likely due to the large dihedral angles between the DHPP-Ph units (\sim 35°). Notably, calculated dihedral angles are consistent with previous electronic structure calculations as well as dihedral angles found for published DHPP crystal structures, thus supporting our level of theory. 26,27 The frontier molecular orbital maps display the electron density of the HOMO resides mostly on the DHPP unit with modest redistribution to ProDOT in the LUMO. This result supports the notion of DHPP being a highly electron-rich building block, 56 thus motivating investigations of its applicability for electrochemical applications. Calculated UV-vis absorbance spectra of the model oligomer, however, are blue-shifted compared to DHPP-co-ProDOT. This discrepancy motivated the synthesis of a (ProDOT)₂DHPP oligomer to compare theory and experimental results for the DHPP/ProDOT systems. Figure 2 shows the overlaid UV-vis spectra for the calculated oligomer, experimental (ProDOT)₂DHPP, and DHPP-co-ProDOT, where calculated and experimental oligomer UV-vis data are in close agreement (~2% λ_{max}). These results further support our level of theory and indicate the effective conjugation length of DHPP-co-ProDOT is greater than 5 rings, even with a large amount of torsional strain distributed through the polymer backbone.

As shown in Figure 3, DHPP-co-ProDOT absorbs with a $\lambda_{\rm max}^{\rm abs}$ of 448 nm, which is attributed to the $\pi-\pi^*$ transition. The featureless absorbance is indicative of a lack of aggregates present in solution, which means the polymer is well solvated in toluene at this concentration. Upon photoexcitation, DHPP-co-ProDOT emits green light with a $\lambda_{\rm max}^{\rm PL}$ of 505 nm. A Stokes shift of 57 nm reveals a modest degree of structural rearrangement upon photoexcitation. DHPP chromophores have been shown to possess high fluorescence quantum yields, which motivated measuring the fluorescence quantum yield. The solution quantum yield (Φ) of DHPP-co-ProDOT was measured to be 13.9% in toluene, indicating a modest

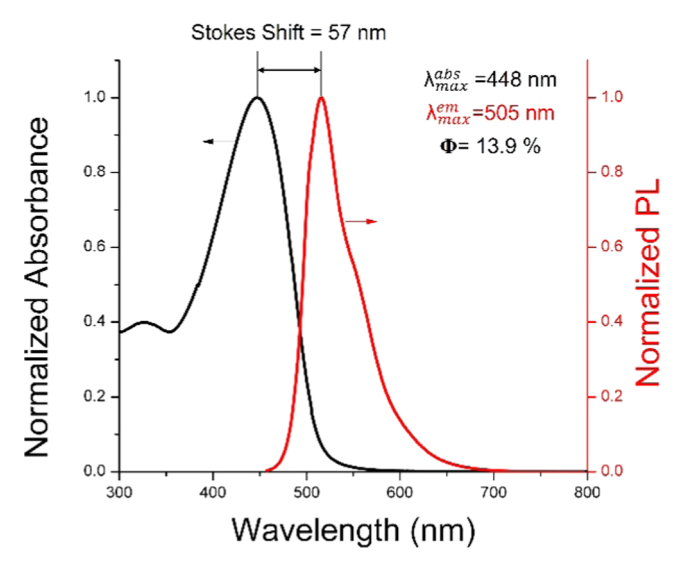


Figure 3. Normalized solution UV–visible absorbance (black) and fluorescence (red) spectra of DHPP-co-ProDOT in toluene solutions with a nominal concentration of $\sim 20~\mu g/mL$.

fluorescence quantum yield. The quantum yield of this DHPP-containing copolymer is notable, as a benchmark value of $\Phi \geq 10\%$ is typically viewed as sufficient for use in organic light-emitting diodes. The DHPP-co-ProDOT exhibited signs of photo-oxidation in solution under ambient conditions after prolonged exposure to sunlight (2 or more weeks). This phenomenon is accelerated for polymers dissolved in chlorinated solvents when irradiated with UV light. Additionally, this photo-oxidation is attributed to the electron-rich properties of the DHPP core in the polymer, facilitating a photoinduced electron transfer (PET) process that has been reported for detecting halocarbons with DHPP chromophores. 58

Initial understanding of DHPP-co-ProDOT thermal properties, such as degradation temperature (T_d) , glass transition $(T_{\rm g})$, and crystallization temperature $(T_{\rm c})$, were studied using thermal gravimetric analysis (TGA) and differential scanning calorimetry (DSC), respectively. TGA was used to determine the degradation temperature of DHPP-co-ProDOT by measuring the mass loss as a function of temperature. Figure S7a shows the TGA trace that indicates DHPP-co-ProDOT has a $T_{\rm d}$ of 377 $^{\circ}\text{C}$ while also providing insight into the purity of the resulting polymer. The absence of degradation and the level trace from r.t. to ~300 °C suggests there are no residual solvents or salts in the polymer and supports our NMR and elemental analysis results. 59 DSC measurements showed no thermal transitions within the experimental range, revealing that the polymer is amorphous in bulk samples (Figure S7b). The absence of thermal transitions is attributed to the large dihedral angles between the pyrrolopyrrole core and benzene rings (~35° as calculated via DFT) that prevent strong interactions between polymer chains and encourage a higher degree of order and crystallinity. Because DHPP-co-ProDOT possesses a high $T_{\rm d}$, it is reasonable to surmise that this polymer can be subjected to postprocessing annealing procedures, if needed, following solution processing.

Due to the electron-rich nature of DHPP and ProDOT, we were motivated to study the redox behavior of DHPP-co-ProDOT as thin films. First, films are spray-cast from 2 mg/mL toluene onto ITO electrodes. The 2 mg/mL concentration

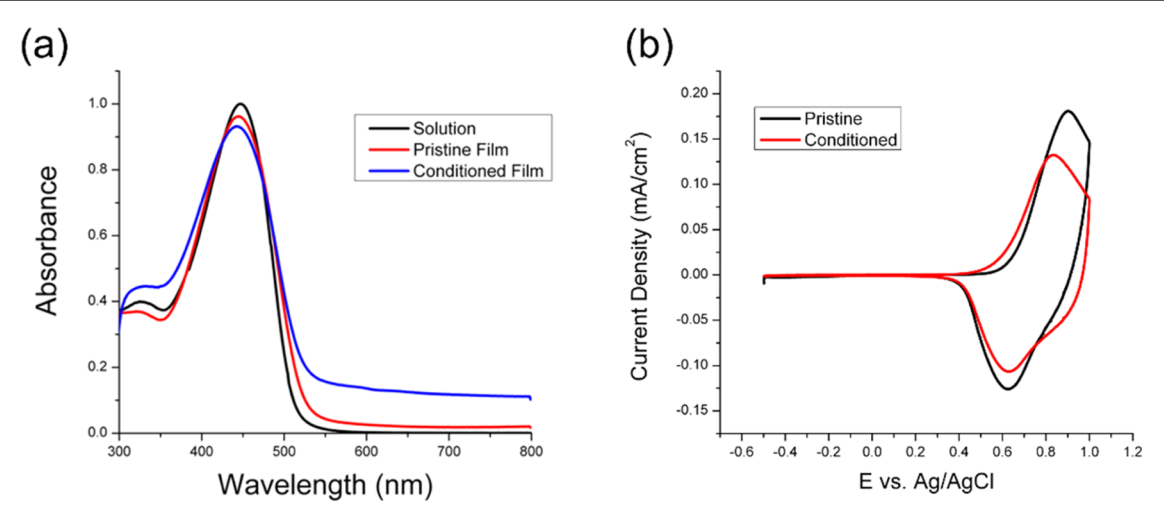


Figure 4. (a) UV–vis absorbance spectra of DHPP-co-ProDOT in solution (black) as a pristine spray-cast film (red) and an electrochemically conditioned film (blue). (b) Cyclic voltammogram traces of DHPP-co-ProDOT as a pristine (black) and electrochemically conditioned film (red). Electrochemical conditioning protocols consist of performing 10 CV cycles across a voltage window of –0.5 to 1.0 V (vs Ag/AgCl reference electrode) in 0.5 M TBAPF₆/PC electrolyte solution using a scan rate of 50 mV/s. UV–vis absorbance spectra were recorded by scanning from 300 to 800 nm.

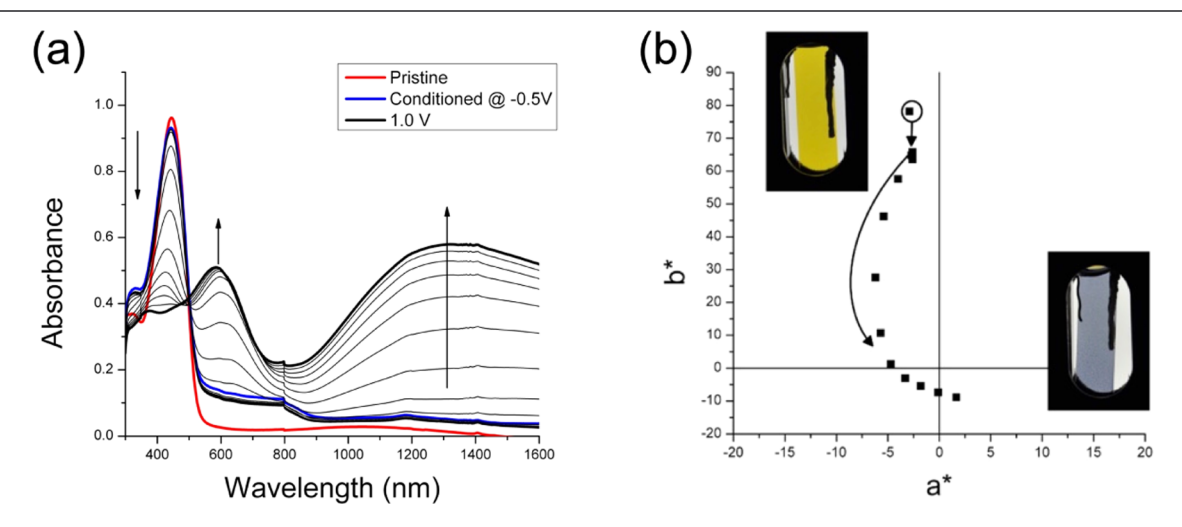


Figure 5. (a) Absorbance spectra as a function of applied potential of a DHPP-co-ProDOT film spray-cast from a 2 mg/mL toluene solution by applying 50 mV potential intervals from -0.5 to 1.0 V in 0.5 M TBAPF₆/PC supporting electrolyte and (b) color coordinates and photographs of a DHPP-co-ProDOT film spray-cast from toluene as a function of applied potential.

appears to be the optimum concentration for this polymer as solutions with higher concentrations or alternative solvents (such as chlorobenzene) were attempted, but adequate solubilities were not achieved. When the UV—vis absorbance spectrum of the resulting film is measured, there is minimal change in the absorbance profile from solution to a pristine film. Typically, conjugated polymers exhibit a distinct red shift in the absorbance spectrum in the solid state when compared to solution due to an increase in $\pi-\pi$ interactions that facilitate ordering. The lack of change in the absorbance spectrum indicates minimal interchain $\pi-\pi$ orbital overlap in the solid state. We attribute this to the large dihedral angles through the polymer backbone that prevent efficient interchain polymer interactions.

After comparing the optical properties of the DHPP-co-ProDOT copolymer in solution and as a pristine film, films are electrochemically conditioned to study the optical properties after subjecting the films to repeated redox reactions. Electrochemical conditioning (EC) is necessary because

redox-active polymers often display distinct changes in their redox response and optical properties with repeated exposure to redox reactions.⁶⁰ EC protocols consist of performing 10 cyclic voltammetry (CV) cycles across a voltage window of -0.5 to 1.0 V (vs Ag/AgCl reference electrode) in a 0.5 M TBAPF₆/PC electrolyte solution using a scan rate of 100 mV/ s. Upon electrochemical conditioning, there is only a slight broadening of the absorbance profile, and the λ_{max} is unchanged (Figure 4a). This observation is rare since conjugated polymers typically exhibit distinct changes in the absorbance spectrum after being subjected to a flux of solvent and ions through the film. Moreover, this finding supports the notion that the polymer is in a disordered state, and EC does not lead to a change in the effective conjugation length, 55 which is typically attributed to the observed changes in the absorbance spectrum of conjugated polymers after repeated redox cycling.

Next, the electrochemical properties were studied using CV. As shown in Figure 4b, despite DHPP-co-ProDOT possessing

large dihedral angles distributed through the backbone, the polymer displays a relatively low onset of oxidation (~0.6 V vs Ag/AgCl). This redox response is analogous to arylene-based copolymers used to access high-gap electrochromic polymers 61,62 but lower than triphenylamine-based copolymers. 63-65 Additionally, the minimal change in absorbance from pristine to conditioned film is confirmed with CV. As seen in Figure 4b, DHPP-co-ProDOT exhibits a quasireversible oxidation and reduction both as pristine and conditioned film, where the onset of oxidation is slightly lower in the conditioned film (~0.6 V vs Ag/AgCl). In contrast, the reduction peak is unchanged after electrochemical conditioning. Another observation is the increased slope of the CV trace between pristine and conditioned films when reducing the film from 1.0 to 0.8 V. This increase is indicative of solvent and ions moving through the film more rapidly due to more accessible redox sites being available.

The reversible and stable redox activity motivates studying absorbance as a function of electrochemical potential, and the results are plotted in Figure 5a. As shown, the π - π * transition at ~448 nm decreases with increasing electrochemical potential, and two new transitions evolve. According to simulation results, both are due to the formation of a radical cation, ⁶⁶ with one species broadly absorbing across the visible spectrum and the second in the IR portion of the electromagnetic spectrum with a maximum absorbance at ~1300 nm (see Supporting Information). Both grow continuously with increasing electrochemical potential.

Colorimetric analysis of polymer films was subsequently performed based on the "Commission Internationale de l'Eclairage" 1976 L*a*b* color standards. Colorimetry data shown in Figure 5b indicates that DHPP-co-ProDOT shows a vibrant yellow color as a neutral film, with a large b^* (~68) and small a^* (\sim -3), which agrees with the absorbance in the high-energy portion of the visible spectrum (400–500 nm). Additionally, colorimetry confirms the minimal changes between pristine (circled) and electrochemically conditioned films observed in the UV-vis absorbance spectrum as evident by only a small decrease in the b^* value while the a^* value remained constant. As the oxidation potential is increased, the b* values begin to decrease, which corresponds to the evolution of the broadly absorbing oxidized species. While b* values decrease, a* values track slightly more negative before returning toward the graph's origin. This color track toward the green portion of the color space is due to the pseudo-dual-band absorbance character between the diminishing π - π * transition and evolving absorbance \sim 600 nm. As the broad absorbance features continue to evolve (Figure S8a), a* and b^* coordinates track to the color-neutral portion of the a*b* plot (Figure S8b).⁶⁷ The color neutrality manifests itself as a black film in the oxidized state, as shown in the photograph presented in Figure 5b.

The long-term electrochemical stability was measured by applying square wave potential steps from -0.5 to 1.0 V vs Ag/AgCl to switch films under an argon atmosphere. As shown in Figure S9, DHPP-co-ProDOT films maintain \sim 95% of contrast after 200 switching cycles but lose 25% of contrast retention after 1000 cycles. The loss of contrast is likely caused by open sites on the phenylene units of the polymer repeat unit that are susceptible to substitution when oxidized or the polymer film requiring an increased break-in period. Regardless, this serves as an area of improvement and motivates further design motifs to improve long-term redox stability.

The overarching goal of this project was to demonstrate the utility of DHPP as a useful building block for simplifying the synthesis of conjugated polymers. The synthetic complexity (SC) can be quantified using the equation developed by Po and co-workers, which is notated as eq 1 and provides a reasonable starting point for comparing the synthetic complexity of DHPP-co-ProDOT to the field. In eq 1, the 5 variables are defined as the number of synthetic steps (NSS), the reciprocal yield of monomers (RY), the number of operations required for purification of monomers (NUO), the number of column chromatography purifications (NCC), and the number of hazardous materials used (NHC), all of which are assigned a weighted value based on the influence each step has on potential cost implications, such as personnel or waste disposal.

$$SC = 35 \frac{NSS}{NSS_{max}} + 25 \frac{\log(RY)}{\log(RY_{max})} + 15 \frac{NUO}{NUO_{max}} + 15 \frac{NCC}{NCC_{max}} + 10 \frac{NHC}{NHC_{max}}$$
(1)

As shown in entry 5 of Table 1, the SC of DHPP-co-ProDOT is calculated to be 13.8, and this represents a synthetically

Table 1. Synthetic Complexity Analysis of Selected Conjugated Polymers and DHPP-co-ProDOT^a

| entry | polymer | NSS | RY | NUO | NCC | NHC | SC |
|-------|----------------------|-----|-----|-----|-----|-----|------|
| 1 | P3HT | 3 | 1.1 | 4 | 0 | 4 | 7.8 |
| 2 | PTQ10 | 3 | 1.1 | 5 | 1 | 6 | 9.7 |
| 3 | cost-effective PTQ10 | 5 | 2.1 | 8 | 1 | 9 | 18.4 |
| 4 | poly(ProDOT) | 5 | 3.1 | 1 | 4 | 9 | 21.3 |
| 5 | DHPP-co-ProDOT | 3 | 3.1 | 0 | 1 | 7 | 13.8 |

"For a comprehensive tabulation of synthetic complexity for conjugated polymers, readers are directed to the work described in ref 5.

simple conjugated polymer. For example, poly(3-hexylthiophene) (P3HT) (entry 1, Table 1) has a synthetic complexity value of 7.8 but is hampered by using Grignard reagents and ultimately possessing modest device performance metrics. 68,69 The synthetic complexity of PTQ10 (entry 2, Table 1) is also calculated to be synthetically simple due to the minimization of preparatory steps. Notably, when calculating the synthetic complexity of the proposed cost-effective route for PTQ10 reported by You and co-workers (entry 3, Table 1),12 the addition of synthetic steps leads to nearly doubling of the synthetic complexity compared to the original synthetic strategy and results in a copolymer more synthetically complex than our DHPP-co-ProDOT. While both PTQ10 approaches still represent simple synthetic strategies for conjugated polymers, Stille cross-coupling polymerizations are used in both studies, which may be detrimental to scalability efforts due to the generation of stoichiometric amounts of toxic waste. Finally, given the potential applicability in redox applications, the SC of DHPP-co-ProDOT is compared to poly(ProDOT) (SC = 21.3, entry 4, Table 1), and DHPP-co-ProDOT is calculated to be less synthetically complex than poly-(ProDOT). Encouragingly, when compared to the extensive analysis of synthetic complexity provided by Po and coworkers, DHPP-co-ProDOT is less synthetically complex than all but two conjugated polymers analyzed in their work. Combined, we have demonstrated DHPP as a viable monomer to simplify the synthesis of conjugated polymers for,

potentially, both solid-state and redox applications. While DHPP-co-ProDOT is not the most synthetically simple conjugated polymer, being able to remove toxic reagents (tin) and air/moisture sensitive reagents (Grignards) shows DHPP-containing copolymers offer significant advantages compared to other conjugated systems.

CONCLUSIONS

Discovering new monomers that efficiently participate in polymerization protocols while simultaneously lowering the synthetic complexity is required for the continued development of the field of conjugated polymers. It is essential to minimize synthetic steps while also removing toxic and air/ moisture-sensitive reagents during synthetic procedures. This study accomplishes these goals by demonstrating the first example of a DHPP comonomer being directly incorporated into the main chain of a polymer repeat unit and providing foundational structure-property relationships of a novel class of polymeric material. Dibrominated DHPP comonomers are synthesized in one aerobic synthesis, purified via vacuum filtration, and are amendable to scalable preparations without sacrificing the purity required for efficient polymerizations. DHPP monomers are successfully incorporated into an electroactive conjugated polymer via direct arylation polymerization with a ProDOT comonomer, which enables studying monomer influence on properties such as degradation temperature, absorbance and fluorescence, and oxidation potential. TD-DFT aids in explaining the wide band gap absorbance features as well as the amorphous nature of the polymer in bulk and thin film samples by understanding the influence of dihedral angles on these properties. Electrochemical studies revealed the quasi-reversible redox nature of DHPP-co-ProDOT as a thin film that displays yellow-to-black electrochromism with a relatively low oxidation potential (~0.6 V vs Ag/AgCl). DHPP successfully demonstrates the feasibility of generating electroactive materials while reducing the number of synthetic steps with relatively benign reagents. This study provides a new approach for simplifying the synthetic complexity commonly associated with generating conjugated polymers while also expanding the synthetic toolbox for the field of conjugated polymers. These findings motivate future investigations into expanding DHPP copolymer design motifs with the goal of improving sustainability of organic electronic materials.

ASSOCIATED CONTENT

Solution Supporting Information

The Supporting Information is available free of charge at https://pubs.acs.org/doi/10.1021/acs.chemmater.2c01884.

Materials and methods, computational details, synthetic procedures, ¹H and ¹³C of monomers and polymers, size-exclusion chromatography, and chronoabsorptometry data (PDF)

AUTHOR INFORMATION

Corresponding Author

Graham S. Collier — Department of Chemistry and Biochemistry, Kennesaw State University, Kennesaw, Georgia 30144, United States; orcid.org/0000-0002-9650-8110; Email: gcollie6@kennesaw.edu

Authors

Kenneth-John J. Bell – Department of Chemistry and Biochemistry, Kennesaw State University, Kennesaw, Georgia 30144, United States

Allison M. Kisiel – Department of Chemistry and Biochemistry, Kennesaw State University, Kennesaw, Georgia 30144. United States

Evan Smith – Department of Chemistry and Biochemistry, University of North Georgia, Dahlonega, Georgia 30597, United States

Aimée L. Tomlinson – Department of Chemistry and Biochemistry, University of North Georgia, Dahlonega, Georgia 30597, United States; orcid.org/0000-0002-6953-4970

Complete contact information is available at: https://pubs.acs.org/10.1021/acs.chemmater.2c01884

Notes

The authors declare no competing financial interest.

ACKNOWLEDGMENTS

The authors acknowledge funding from the Department of Chemistry and Biochemistry at Kennesaw State University through departmental start-up funds. This material is based upon work supported by the National Science Foundation under Grant No. 2203340. The College of Science and Mathematics is also acknowledged for funding through the Mentor-Protégé Research Program as well as facilitating the Birla Carbon Scholars Program, a summer undergraduate research experience made possible thanks to the generous donation from Birla Carbon. The authors also acknowledge funding from the Office of Undergraduate Research at Kennesaw State University for the Undergraduate Research and Creative Activities (URCA) funds. The authors would like to acknowledge Kennesaw State University Academic Affairs for support of the NMR facility, which made possible the research necessary for the completion of this project. The Reynolds Research Group at Georgia Tech is acknowledged for generous access to film processing and characterization facilities. The authors thank the National Science Foundation's Extreme Science and Engineering Discovery (NSF XSEDE, DMR 160146) and the San Diego Supercomputer Center for providing access to their Expanse cluster, without which the TD-DFT computations could not have been completed in a timely fashion.

REFERENCES

- (1) Lu, L.; Zheng, T.; Wu, Q.; Schneider, A. M.; Zhao, D.; Yu, L. Recent Advances in Bulk Heterojunction Polymer Solar Cells. *Chem. Rev.* **2015**, *115*, 12666–12731.
- (2) Salehi, A.; Fu, X.; Shin, D.-H.; So, F. Recent Advances in OLED Optical Design. *Adv. Funct. Mater.* **2019**, 29, No. 1808803.
- (3) Li, X.; Perera, K.; He, J.; Gumyusenge, A.; Mei, J. Solution-Processable Electrochromic Materials and Devices: Roadblocks and Strategies Towards Large-Scale Applications. *J. Mater. Chem. C* **2019**, 7, 12761–12789.
- (4) Osedach, T. P.; Andrew, T. L.; Bulović, V. Effect of Synthetic Accessibility on the Commercial Viability of Organic Photovoltaics. *Energy Environ. Sci.* **2013**, *6*, 711–718.
- (5) Po, R.; Bianchi, G.; Carbonera, C.; Pellegrino, A. All That Glisters Is Not Gold": An Analysis of the Synthetic Complexity of Efficient Polymer Donors for Polymer Solar Cells. *Macromolecules* **2015**, *48*, 453–461.

- (6) Li, X.; Pan, F.; Sun, C.; Zhang, M.; Wang, Z.; Du, J.; Wang, J.; Xiao, M.; Xue, L.; Zhang, Z.-G.; Zhang, C.; Liu, F.; Li, Y. Simplified Synthetic Routes for Low Cost and High Photovoltaic Performance N-Type Organic Semiconductor Acceptors. *Nat. Commun.* **2019**, *10*, No. 519.
- (7) Moser, M.; Wadsworth, A.; Gasparini, N.; McCulloch, I. Challenges to the Success of Commercial Organic Photovoltaic Products. *Adv. Energy Mater.* **2021**, *11*, No. 2100056.
- (8) Min, J.; Luponosov, Y. N.; Cui, C.; Kan, B.; Chen, H.; Wan, X.; Chen, Y.; Ponomarenko, S. A.; Li, Y.; Brabec, C. J. Evaluation of Electron Donor Materials for Solution-Processed Organic Solar Cells via a Novel Figure of Merit. *Adv. Energy Mater.* **2017**, *7*, No. 1700465.
- (9) Sun, C.; Pan, F.; Bin, H.; Zhang, J.; Xue, L.; Qiu, B.; Wei, Z.; Zhang, Z.-G.; Li, Y. A Low Cost and High Performance Polymer Donor Material for Polymer Solar Cells. *Nat. Commun.* **2018**, *9*, No. 743.
- (10) Li, S.; Zhan, L.; Sun, C.; Zhu, H.; Zhou, G.; Yang, W.; Shi, M.; Li, C.-Z.; Hou, J.; Li, Y.; Chen, H. Highly Efficient Fullerene-Free Organic Solar Cells Operate at Near Zero Highest Occupied Molecular Orbital Offsets. *J. Am. Chem. Soc.* **2019**, *141*, 3073–3082.
- (11) Sun, C.; Qin, S.; Wang, R.; Chen, S.; Pan, F.; Qiu, B.; Shang, Z.; Meng, L.; Zhang, C.; Xiao, M.; Yang, C.; Li, Y. High Efficiency Polymer Solar Cells with Efficient Hole Transfer at Zero Highest Occupied Molecular Orbital Offset between Methylated Polymer Donor and Brominated Acceptor. *J. Am. Chem. Soc.* **2020**, *142*, 1465–1474.
- (12) Rech, J. J.; Neu, J.; Qin, Y.; Samson, S.; Shanahan, J.; Josey, R. F.; Ade, H.; You, W. Designing Simple Conjugated Polymers for Scalable and Efficient Organic Solar Cells. *ChemSusChem* **2021**, *14*, 3561–3568.
- (13) Zhang, M.; Guo, X.; Ma, W.; Ade, H.; Hou, J. A Polythiophene Derivative with Superior Properties for Practical Application in Polymer Solar Cells. *Adv. Mater.* **2014**, *26*, 5880–5885.
- (14) Qin, Y.; Uddin, M. A.; Chen, Y.; Jang, B.; Zhao, K.; Zheng, Z.; Yu, R.; Shin, T. J.; Woo, H. Y.; Hou, J. Highly Efficient Fullerene-Free Polymer Solar Cells Fabricated with Polythiophene Derivative. *Adv. Mater.* **2016**, 28, 9416–9422.
- (15) Ko, S.-J.; Hoang, Q. V.; Song, C. E.; Uddin, M. A.; Lim, E.; Park, S. Y.; Lee, B. H.; Song, S.; Moon, S.-J.; Hwang, S.; Morin, P.-O.; Leclerc, M.; Su, G. M.; Chabinyc, M. L.; Woo, H. Y.; Shin, W. S.; Kim, J. Y. High-Efficiency Photovoltaic Cells with Wide Optical Band Gap Polymers Based on Fluorinated Phenylene-Alkoxybenzothiadiazole. *Energy Environ. Sci.* **2017**, *10*, 1443–1455.
- (16) Zhao, J.; Li, Y.; Yang, G.; Jiang, K.; Lin, H.; Ade, H.; Ma, W.; Yan, H. Efficient Organic Solar Cells Processed from Hydrocarbon Solvents. *Nat. Energy* **2016**, *1*, 15027.
- (17) Yao, H.; Cui, Y.; Qian, D.; Ponseca, C. S.; Honarfar, A.; Xu, Y.; Xin, J.; Chen, Z.; Hong, L.; Gao, B.; Yu, R.; Zu, Y.; Ma, W.; Chabera, P.; Pullerits, T.; Yartsev, A.; Gao, F.; Hou, J. 14.7% Efficiency Organic Photovoltaic Cells Enabled by Active Materials with a Large Electrostatic Potential Difference. *J. Am. Chem. Soc.* **2019**, *141*, 7743–7750.
- (18) Jeon, S. J.; Han, Y. W.; Moon, D. K. Chlorine Effects of Heterocyclic Ring-Based Donor Polymer for Low-Cost and High-Performance Nonfullerene Polymer Solar Cells. *Sol. RRL* **2019**, 3, No. 1900094.
- (19) Pankow, R. M.; Wu, J.; Harbuzaru, A.; Kerwin, B.; Chen, Y.; Ortiz, R. P.; Facchetti, A.; Marks, T. J. All-Polymer Solar Cells Incorporating Readily Accessible Naphthalene Diimide and Isoindigo Acceptor Polymers for Improved Light Harvesting. *Chem. Mater.* 2022, 34, 3267–3279.
- (20) Krzeszewski, M.; Gryko, D.; Gryko, D. T. The Tetraarylpyrrolo[3,2-b]Pyrroles—From Serendipitous Discovery to Promising Heterocyclic Optoelectronic Materials. *Acc. Chem. Res.* **2017**, *50*, 2334–2345.
- (21) Janiga, A.; Glodkowska-Mrowka, E.; Stoklosa, T.; Gryko, D. T. Synthesis and Optical Properties of Tetraaryl-1,4-Dihydropyrrolo[3,2-b]Pyrroles. *Asian J. Org. Chem.* **2013**, *2*, 411–415.

- (22) Krzeszewski, M.; Thorsted, B.; Brewer, J.; Gryko, D. T. Tetraaryl-, Pentaaryl-, and Hexaaryl-1,4-Dihydropyrrolo[3,2-b]-Pyrroles: Synthesis and Optical Properties. *J. Org. Chem.* **2014**, *79*, 3119–3128.
- (23) Tasior, M.; Koszarna, B.; Young, D. C.; Bernard, B.; Jacquemin, D.; Gryko, D.; Gryko, D. T. Fe(III)-Catalyzed Synthesis of Pyrrolo[3,2-b]Pyrroles: Formation of New Dyes and Photophysical Studies. *Org. Chem. Front.* **2019**, *6*, 2939–2948.
- (24) Tasior, M.; Vakuliuk, O.; Koga, D.; Koszarna, B.; Górski, K.; Grzybowski, M.; Kielesiński, Ł.; Krzeszewski, M.; Gryko, D. T. Method for the Large-Scale Synthesis of Multifunctional 1,4-Dihydro-Pyrrolo [3,2-b] Pyrroles. *J. Org. Chem.* **2020**, *85*, 13529–13543.
- (25) Tasior, M.; Clermont, G.; Blanchard-Desce, M.; Jacquemin, D.; Gryko, D. T. Synthesis of Bis(Arylethynyl)Pyrrolo[3,2-b]Pyrroles and Effect of Intramolecular Charge Transfer on Their Photophysical Behavior. *Chem. Eur. J.* **2019**, *25*, 598–608.
- (26) Banasiewicz, M.; Stężycki, R.; Kumar, G. D.; Krzeszewski, M.; Tasior, M.; Koszarna, B.; Janiga, A.; Vakuliuk, O.; Sadowski, B.; Gryko, D. T.; Jacquemin, D. Electronic Communication in Pyrrolo-[3,2-b]Pyrroles Possessing Sterically Hindered Aromatic Substituents. *Eur. J. Org. Chem.* **2019**, 2019, 5247–5253.
- (27) Sadowski, B.; Hassanein, K.; Ventura, B.; Gryko, D. T. Tetraphenylethylenepyrrolo[3,2-b]Pyrrole Hybrids as Solid-State Emitters: The Role of Substitution Pattern. *Org. Lett.* **2018**, *20*, 3183–3186.
- (28) Hatanaka, S.; Ono, T.; Yano, Y.; Gryko, D. T.; Hisaeda, Y. Tris(Pentafluorophenyl)Borane-Pyrrolo[3,2-b]Pyrrole Hybrids: Solid-State Structure and Crystallization-Induced Enhanced Emission. *ChemPhotoChem* **2020**, *4*, 138–143.
- (29) Qin, Y.; Schnedermann, C.; Tasior, M.; Gryko, D. T.; Nocera, D. G. Direct Observation of Different One- and Two-Photon Fluorescent States in a Pyrrolo[3,2-b]Pyrrole Fluorophore. *J. Phys. Chem. Lett.* **2020**, *11*, 4866–4872.
- (30) Domínguez, R.; Montcada, N. F.; de la Cruz, P.; Palomares, E.; Langa, F. Pyrrolo[3,2-b]Pyrrole as the Central Core of the Electron Donor for Solution-Processed Organic Solar Cells. *ChemPlusChem* **2017**, 82, 1096–1104.
- (31) Wang, J.; Chai, Z.; Liu, S.; Fang, M.; Chang, K.; Han, M.; Hong, L.; Han, H.; Li, Q.; Li, Z. Organic Dyes Based on Tetraaryl-1,4-Dihydropyrrolo-[3,2-b]Pyrroles for Photovoltaic and Photocatalysis Applications with the Suppressed Electron Recombination. *Chem. Eur. J.* 2018, 24, 18032–18042.
- (32) Zhou, Y.; Zhang, M.; Ye, J.; Liu, H.; Wang, K.; Yuan, Y.; Du, Y.-Q.; Zhang, C.; Zheng, C.-J.; Zhang, X.-H. Efficient Solution-Processed Red Organic Light-Emitting Diode Based on an Electron-Donating Building Block of Pyrrolo[3,2-b]Pyrrole. *Org. Electron.* **2019**, *6S*, 110–115.
- (33) Balasubramanyam, R. K. C.; Kumar, R.; Ippolito, S. J.; Bhargava, S. K.; Periasamy, S. R.; Narayan, R.; Basak, P. Quadrupolar (A-π-D-π-A) Tetra-Aryl 1,4-Dihydropyrrolo[3,2-b]Pyrroles as Single Molecular Resistive Memory Devices: Substituent Triggered Amphoteric Redox Performance and Electrical Bistability. *J. Phys. Chem. C* **2016**, *120*, 11313–11323.
- (34) Balasubramanyam, R. K. C.; Kandjani, A. E.; Harrison, C. J.; Abdul Haroon Rashid, S. S. A.; Sabri, Y. M.; Bhargava, S. K.; Narayan, R.; Basak, P.; Ippolito, S. J. 1,4-Dihydropyrrolo[3,2-b]Pyrroles as a Single Component Photoactive Layer: A New Paradigm for Broadband Detection. ACS Appl. Mater. Interfaces 2017, 9, 27875—27882.
- (35) Sakamoto, J.; Rehahn, M.; Wegner, G.; Schlüter, A. D. Suzuki Polycondensation: Polyarylenes à La Carte. *Macromol. Rapid Commun.* **2009**, 30, 653–687.
- (36) Carsten, B.; He, F.; Son, H. J.; Xu, T.; Yu, L. Stille Polycondensation for Synthesis of Functional Materials. *Chem. Rev.* **2011**. *111*. 1493–1528.
- (37) Mainville, M.; Leclerc, M. Direct (Hetero)Arylation: A Tool for Low-Cost and Eco-Friendly Organic Photovoltaics. *ACS Appl. Polym. Mater.* **2021**, 3, 2–13.

- (38) Blaskovits, J. T.; Leclerc, M. C-H Activation as a Shortcut to Conjugated Polymer Synthesis. *Macromol. Rapid Commun.* **2019**, 40, No. 1800512.
- (39) Pouliot, J.-R.; Grenier, F.; Blaskovits, J. T.; Beaupré, S.; Leclerc, M. Direct (Hetero)Arylation Polymerization: Simplicity for Conjugated Polymer Synthesis. *Chem. Rev.* **2016**, *116*, 14225–14274.
- (40) Pankow, R. M.; Thompson, B. C. The Development of Conjugated Polymers as the Cornerstone of Organic Electronics. *Polymer* **2020**, 207, No. 122874.
- (41) Ponder, J. F., Jr.; Chen, H.; Luci, A. M. T.; Moro, S.; Turano, M.; Hobson, A. L.; Collier, G. S.; Perdigão, L. M. A.; Moser, M.; Zhang, W.; Costantini, G.; Reynolds, J. R.; McCulloch, I. Low-Defect, High Molecular Weight Indacenodithiophene (IDT) Polymers Via a C–H Activation: Evaluation of a Simpler and Greener Approach to Organic Electronic Materials. ACS Mater. Lett. 2021, 3, 1503–1512.
- (42) Pron, A.; Berrouard, P.; Leclerc, M. Thieno[3,4-c]Pyrrole-4,6-Dione-Based Polymers for Optoelectronic Applications. *Macromol. Chem. Phys.* **2013**, 214, 7–16.
- (43) Collier, G. S.; Reynolds, J. R. Exploring the Utility of Buchwald Ligands for C–H Oxidative Direct Arylation Polymerizations. *ACS Macro Lett.* **2019**, *8*, 931–936.
- (44) Reeves, B. D.; Grenier, C. R. G.; Argun, A. A.; Cirpan, A.; McCarley, T. D.; Reynolds, J. R. Spray Coatable Electrochromic Dioxythiophene Polymers with High Coloration Efficiencies. *Macromolecules* **2004**, *37*, 7559–7569.
- (45) Dey, T.; Invernale, M. A.; Ding, Y.; Buyukmumcu, Z.; Sotzing, G. A. Poly(3,4-Propylenedioxythiophene)s as a Single Platform for Full Color Realization. *Macromolecules* **2011**, *44*, 2415–2417.
- (46) Mazaheripour, A.; Thomas, E. M.; Segalman, R. A.; Chabinyc, M. L. Nonaggregating Doped Polymers Based on Poly(3,4-Propylenedioxythiophene. *Macromolecules* **2019**, *52*, 2203–2213.
- (47) Thompson, B. C.; Kim, Y.-G.; McCarley, T. D.; Reynolds, J. R. Soluble Narrow Band Gap and Blue Propylenedioxythiophene-Cyanovinylene Polymers as Multifunctional Materials for Photovoltaic and Electrochromic Applications. J. Am. Chem. Soc. 2006, 128, 12714–12725.
- (48) Estrada, L. A.; Deininger, J. J.; Kamenov, G. D.; Reynolds, J. R. Direct (Hetero)Arylation Polymerization: An Effective Route to 3,4-Propylenedioxythiophene-Based Polymers with Low Residual Metal Content. ACS Macro Lett. 2013, 2, 869–873.
- (49) Ryu, H. G.; Mayther, M. F.; Tamayo, J.; Azarias, C.; Espinoza, E. M.; Banasiewicz, M.; Łukasiewicz, Ł. G.; Poronik, Y. M.; Jeżewski, A.; Clark, J.; Derr, J. B.; Ahn, K. H.; Gryko, D. T.; Jacquemin, D.; Vullev, V. I. Bidirectional Solvatofluorochromism of a Pyrrolo[3,2-b]Pyrrole—Diketopyrrolopyrrole Hybrid. *J. Phys. Chem. C* 2018, 122, 13424—13434.
- (50) Culver, E. W.; Anderson, T. E.; López Navarrete, J. T.; Ruiz Delgado, M. C.; Rasmussen, S. C. Poly(Thieno[3,4-b]Pyrazine-Alt-2,1,3-Benzothiadiazole)s: A New Design Paradigm in Low Band Gap Polymers. ACS Macro Lett. 2018, 7, 1215–1219.
- (51) Usluer, Ö.; Abbas, M.; Wantz, G.; Vignau, L.; Hirsch, L.; Grana, E.; Brochon, C.; Cloutet, E.; Hadziioannou, G. Metal Residues in Semiconducting Polymers: Impact on the Performance of Organic Electronic Devices. *ACS Macro Lett.* **2014**, *3*, 1134–1138.
- (52) Curtin, I. J.; Blaylock, D. W.; Holmes, R. J. Role of Impurities in Determining the Exciton Diffusion Length in Organic Semi-conductors. *Appl. Phys. Lett.* **2016**, *108*, No. 163301.
- (53) Bracher, C.; Yi, H.; Scarratt, N. W.; Masters, R.; Pearson, A. J.; Rodenburg, C.; Iraqi, A.; Lidzey, D. G. The Effect of Residual Palladium Catalyst on the Performance and Stability of PCDTBT:PC70BM Organic Solar Cells. *Org. Electron.* **2015**, 27, 266–273.
- (54) Wheeler, D. L.; Rainwater, L. E.; Green, A. R.; Tomlinson, A. L. Modeling Electrochromic Poly-Dioxythiophene-Containing Materials Through TDDFT. *Phys. Chem. Chem. Phys.* **2017**, *19*, 20251–20258. (55) Collier, G. S.; Wilkins, R.; Tomlinson, A. L.; Reynolds, J. R. Exploring Isomeric Effects on Optical and Electrochemical Properties of Red/Orange Electrochromic Polymers. *Macromolecules* **2021**, *54*, 1677–1692.

- (56) Tanaka, S.; Kumagai, T.; Mukai, T.; Kobayashi, T. 1,4-Dihydropyrrolo[3,2-b]Pyrrole: The Electronic Structure Elucidated by Photoelectron Spectroscopy. *Bull. Chem. Soc. Jpn.* **1987**, *60*, 1981–1983.
- (57) Ravindran, E.; Somanathan, N. Efficient White-Light Emission from a Single Polymer System with "Spring-like" Self-Assemblies Induced Emission Enhancement and Intramolecular Charge Transfer Characteristics. *J. Mater. Chem. C* **2017**, *5*, 4763–4774.
- (58) Wu, J.-Y.; Yu, C.-H.; Wen, J.-J.; Chang, C.-L.; Leung, M. Pyrrolo-[3,2-b]Pyrroles for Photochromic Analysis of Halocarbons. *Anal. Chem.* **2016**, *88*, 1195–1201.
- (59) Lo, C. K.; Wolfe, R. M. W.; Reynolds, J. R. From Monomer to Conjugated Polymer: A Perspective on Best Practices for Synthesis. *Chem. Mater.* **2021**, 33, 4842–4852.
- (60) Heinze, J.; Frontana-Uribe, B. A.; Ludwigs, S. Electrochemistry of Conducting Polymers—Persistent Models and New Concepts. *Chem. Rev.* **2010**, *110*, 4724–4771.
- (61) Kerszulis, J. A.; Amb, C. M.; Dyer, A. L.; Reynolds, J. R. Follow the Yellow Brick Road: Structural Optimization of Vibrant Yellow-to-Transmissive Electrochromic Conjugated Polymers. *Macromolecules* **2014**, *47*, 5462–5469.
- (62) Amb, C. M.; Kerszulis, J. A.; Thompson, E. J.; Dyer, A. L.; Reynolds, J. R. Propylenedioxythiophene (ProDOT)—Phenylene Copolymers Allow a Yellow-to-Transmissive Electrochrome. *Polym. Chem.* **2011**, *2*, 812—814.
- (63) Yen, H.-J.; Liou, G.-S. Solution-Processable Triarylamine-Based Electroactive High Performance Polymers for Anodically Electrochromic Applications. *Polym. Chem.* **2012**, *3*, 255–264.
- (64) Beaupré, S.; Dumas, J.; Leclerc, M. Toward the Development of New Textile/Plastic Electrochromic Cells Using Triphenylamine-Based Copolymers. *Chem. Mater.* **2006**, *18*, 4011–4018.
- (65) Jeong, J.; Kumar, R. S.; Naveen, M.; Son, Y.-A. Synthesis and Characterization of Triphenylamine-Based Polymers and Their Application Towards Solid-State Electrochromic Cells. *RSC Adv.* **2016**, *6*, 78984–78993.
- (66) Heimel, G. The Optical Signature of Charges in Conjugated Polymers. ACS Cent. Sci. 2016, 2, 309–315.
- (67) Lo, C. K.; Shen, D. E.; Reynolds, J. R. Fine-Tuning the Color Hue of π -Conjugated Black-to-Clear Electrochromic Random Copolymers. *Macromolecules* **2019**, 52, 6773–6779.
- (68) Baran, D.; Ashraf, R. S.; Hanifi, D. A.; Abdelsamie, M.; Gasparini, N.; Röhr, J. A.; Holliday, S.; Wadsworth, A.; Lockett, S.; Neophytou, M.; Emmott, C. J. M.; Nelson, J.; Brabec, C. J.; Amassian, A.; Salleo, A.; Kirchartz, T.; Durrant, J. R.; McCulloch, I. Reducing the Efficiency–Stability—Cost Gap of Organic Photovoltaics with Highly Efficient and Stable Small Molecule Acceptor Ternary Solar Cells. *Nat. Mater.* **2017**, *16*, 363–369.
- (69) Guo, X.; Cui, C.; Zhang, M.; Huo, L.; Huang, Y.; Hou, J.; Li, Y. High Efficiency Polymer Solar Cells Based on Poly(3-Hexylthiophene)/Indene-C70 Bisadduct with Solvent Additive. *Energy Environ. Sci.* **2012**, *5*, 7943–7949.